Characterizing the Molecular Interstellar Medium in Galaxies using Archival Herschel Data

Naseem Rangwala

University of Colorado - Boulder

NASA Ames Research Center

Main Collaborators: Jason Glenn (CU)
Julia Kamenetzky (CU)
Phil Maloney (CU)

This work is supported by a NASA ADAP grant

Outline

- Description of the program
- Goals
- Sample
- Methodology / Pipeline
- Preliminary Results (spectra, modeling results, CO SLEDs etc.)
- Conclusions

Description of our Archival Program

- Archival (publicly available) survey using photometric and spectroscopic data of all the galaxies (~300) observed with *Herschel*-SPIRE's Fourier Transform Spectrometer (FTS).

SPIRE-FTS spectrum of Arp 220

670 µm ← **300 µm** ← **190 µm**

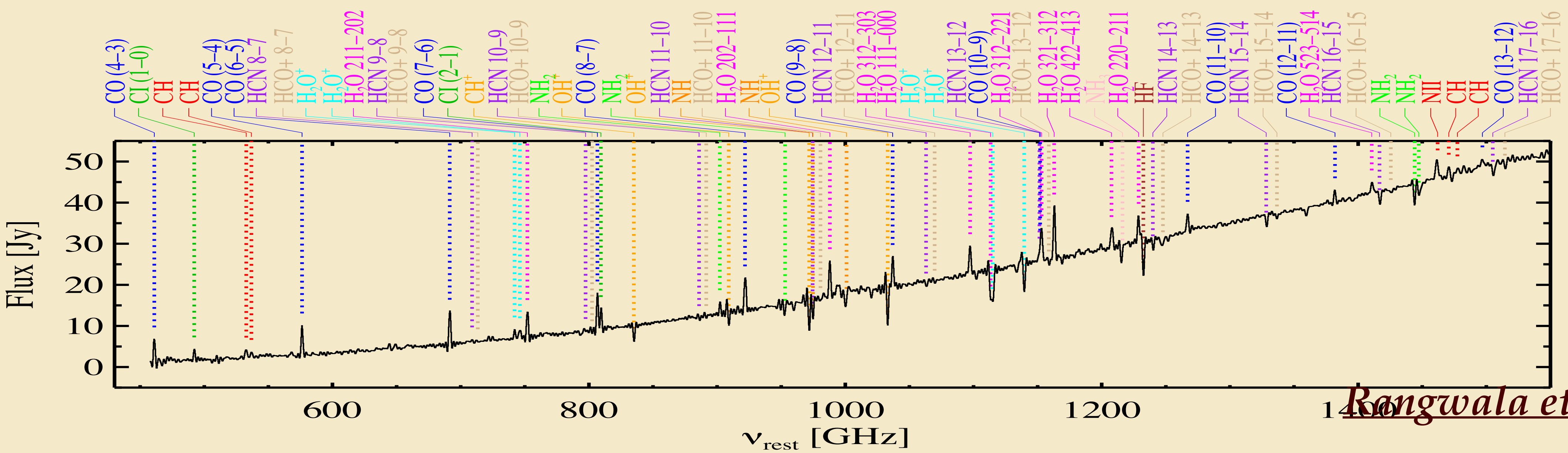

Rangwala et al. (2011)

- Continuous spectral coverage
- several molecular and atomic species
- spectral resolution = 1.44 GHz
- CO rotational transitions from J = 4-3 to 13-12

Description of our Archival Program

- Archival (publicly available) survey using photometric and spectroscopic data of all the galaxies (~300) observed with *Herschel*-SPIRE's Fourier Transform Spectrometer (FTS).
- This sample spans a wide range in the far-infrared luminosity (L_{FIR}) and galaxy types.

SPIRE- FTS Archival Sample

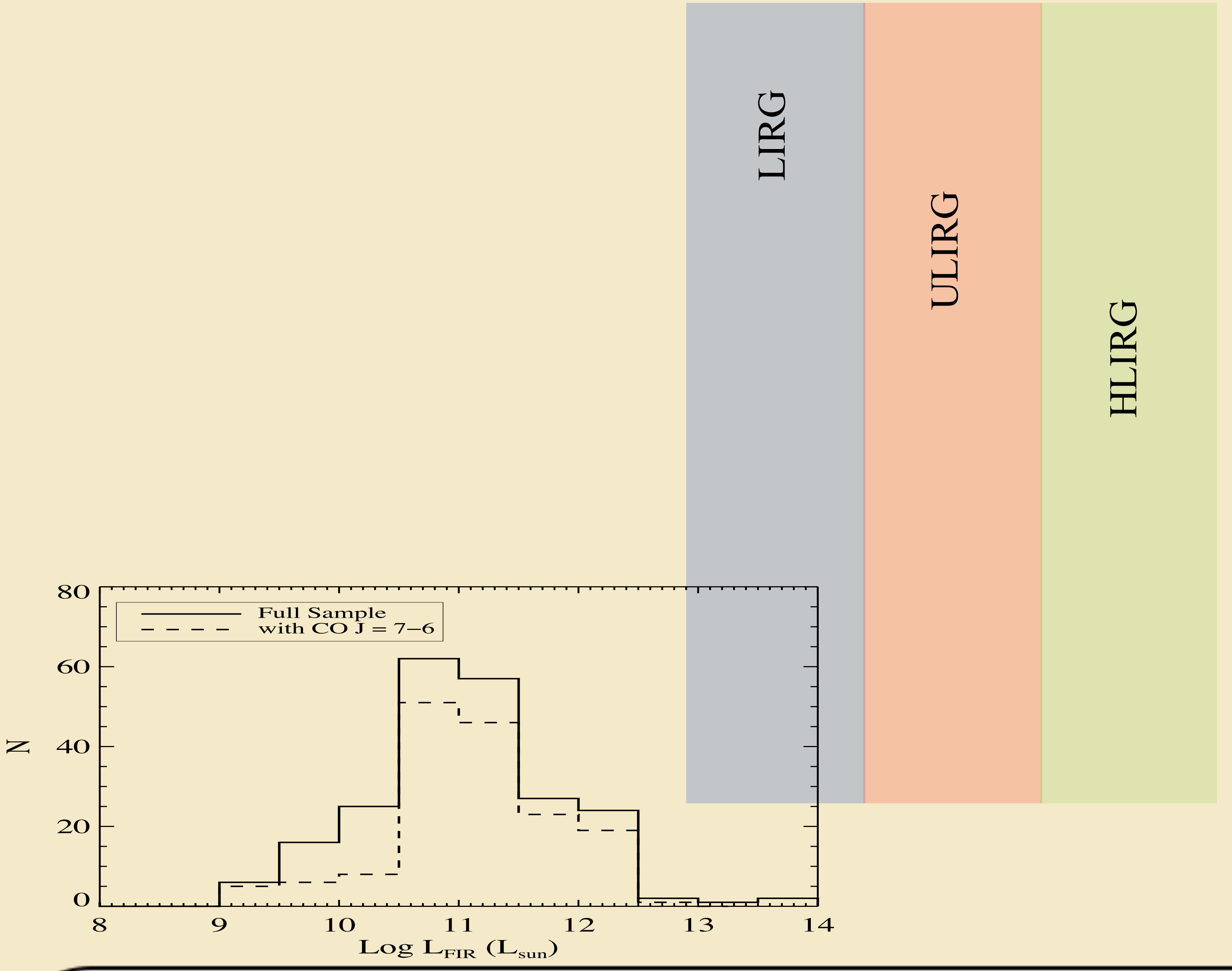

- N_{tot} ~ 300 (AGN = 78, Ellipticals = 32)
- 168/227 galaxies have CO J = 7-6 detection
- redshift up to z = 0.2

Description of our Archival Program

- Archival (publicly available) survey using photometric and spectroscopic data of all the galaxies (~300) observed with *Herschel*-SPIRE's Fourier Transform Spectrometer (FTS).

- This sample span a wide range in the far-infrared luminosity (L_{FIR}) and galaxy types.

- CO spectral line energy distributions (SLEDs) from these spectra will be uniformly re-reduced, re-calibrated and modeled to estimate the physical conditions and reservoir of the molecular gas

- Application of consistent methodology for data reduction and modeling across the entire sample will enable accurate comparison between different galaxies

Goals of the Program

- Determine the molecular gas (and dust) properties as a function of L_{FIR} and galaxy type (starburst, AGN, disks and ellipticals)
- Address the origin of the excitation of warm molecular gas of varying L_{FIR}: Star-Formation vs AGN?
- Compare the gas excitation and dust properties of the local IR luminous galaxies to high-z submm galaxies.
- Explore *Total* L_{CO} - L_{FIR} Relation
- Direct measurement of [CO/H_2] abundance for warm molecular gas.
- Substantial public database of legacy value for nearby galaxies

CO SLED: diagnostic for Star Formation Vs AGN?

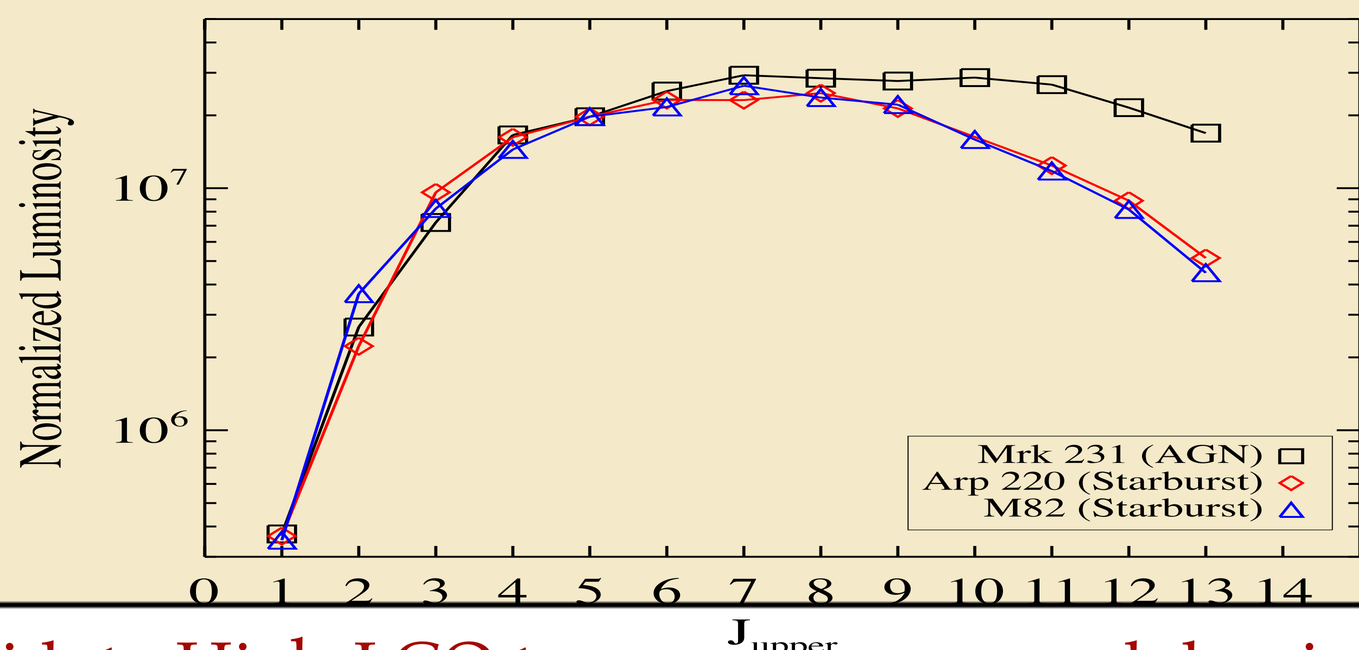

Mid- to High-J CO traces warm gas and dominates the CO luminosity and cooling

Goals of the Program

- Determine the molecular gas (and dust) properties as a function of L_{FIR} and galaxy type (starburst, AGN, disks and ellipticals)

- Address the origin of the excitation of warm molecular gas of varying L_{FIR}: Star-Formation Vs AGN?

- Compare the gas excitation and dust properties of the local IR luminous galaxies to high-z submm galaxies.

- Explore *Total* L_{CO} - L_{FIR} Relation

- Direct measurement of [CO/H_2] abundance for warm molecular gas.

- Substantial public database of legacy value for nearby galaxies

Pipeline Schematic

Pipeline developed by
J. Kamenetzky

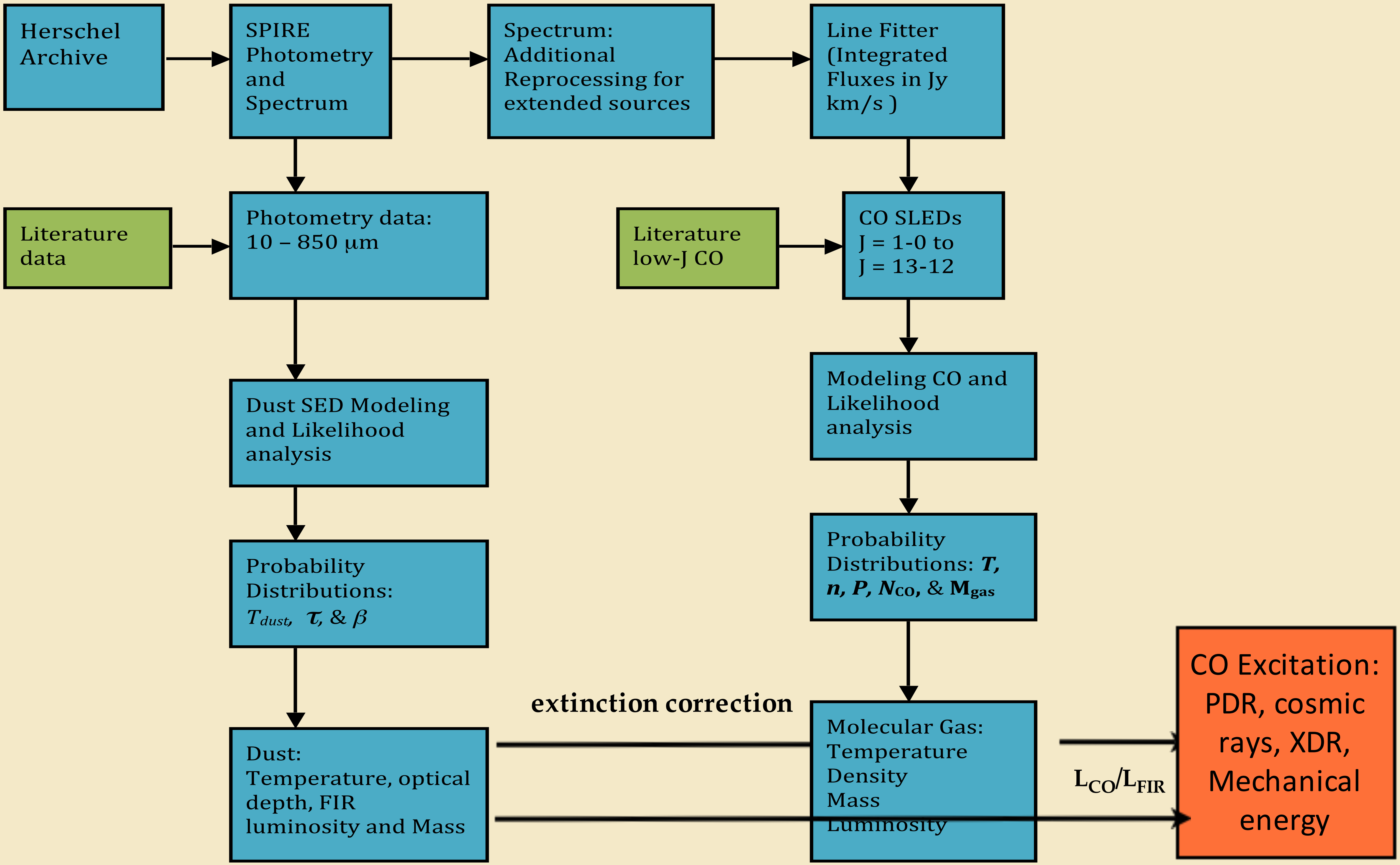

DATA

M82 (Starburst)

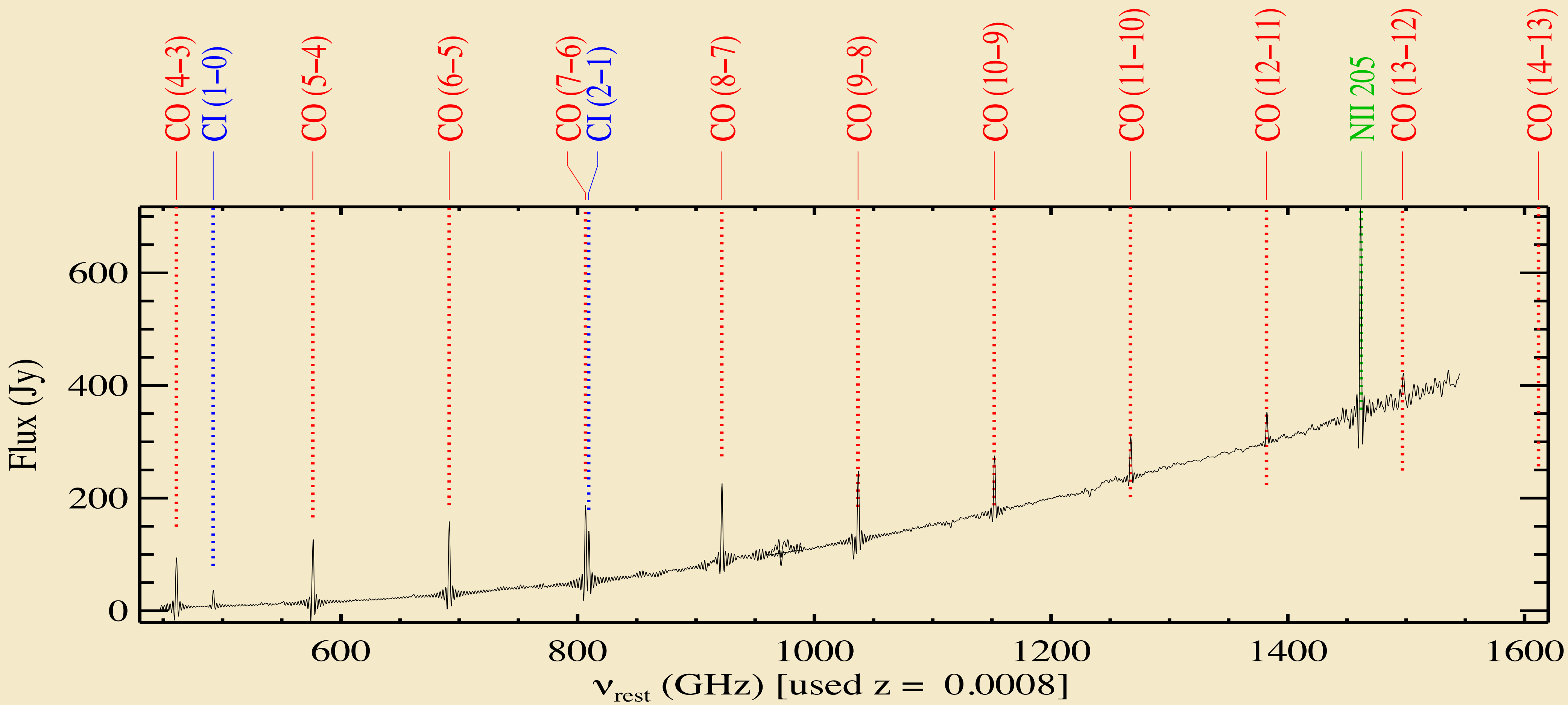

This survey will focus only on CO, CI and NII lines. CO and CI for characterizing molecular gas and NII as a star formation tracer

NGC 6240 (LIRG/AGN)

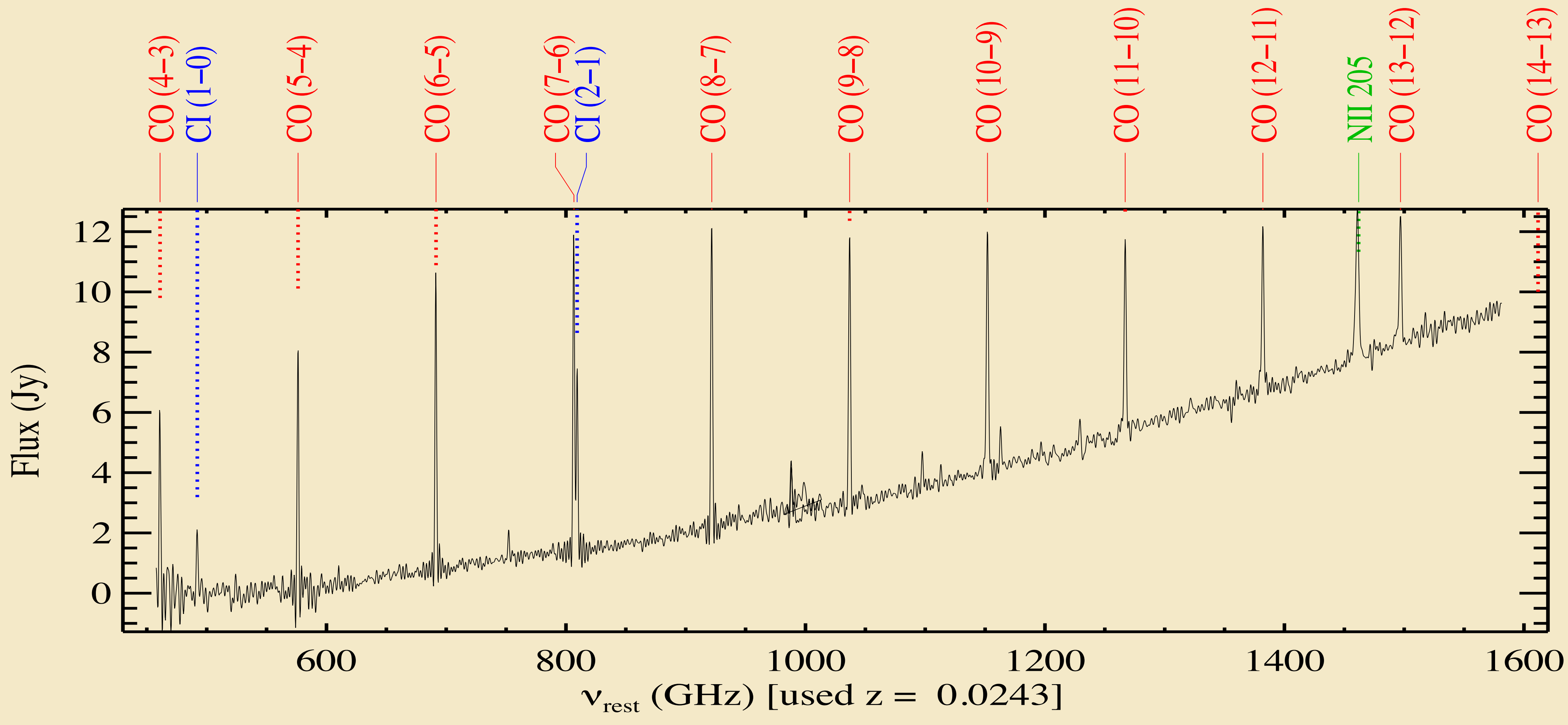

MRK 231 (ULIRG/AGN)

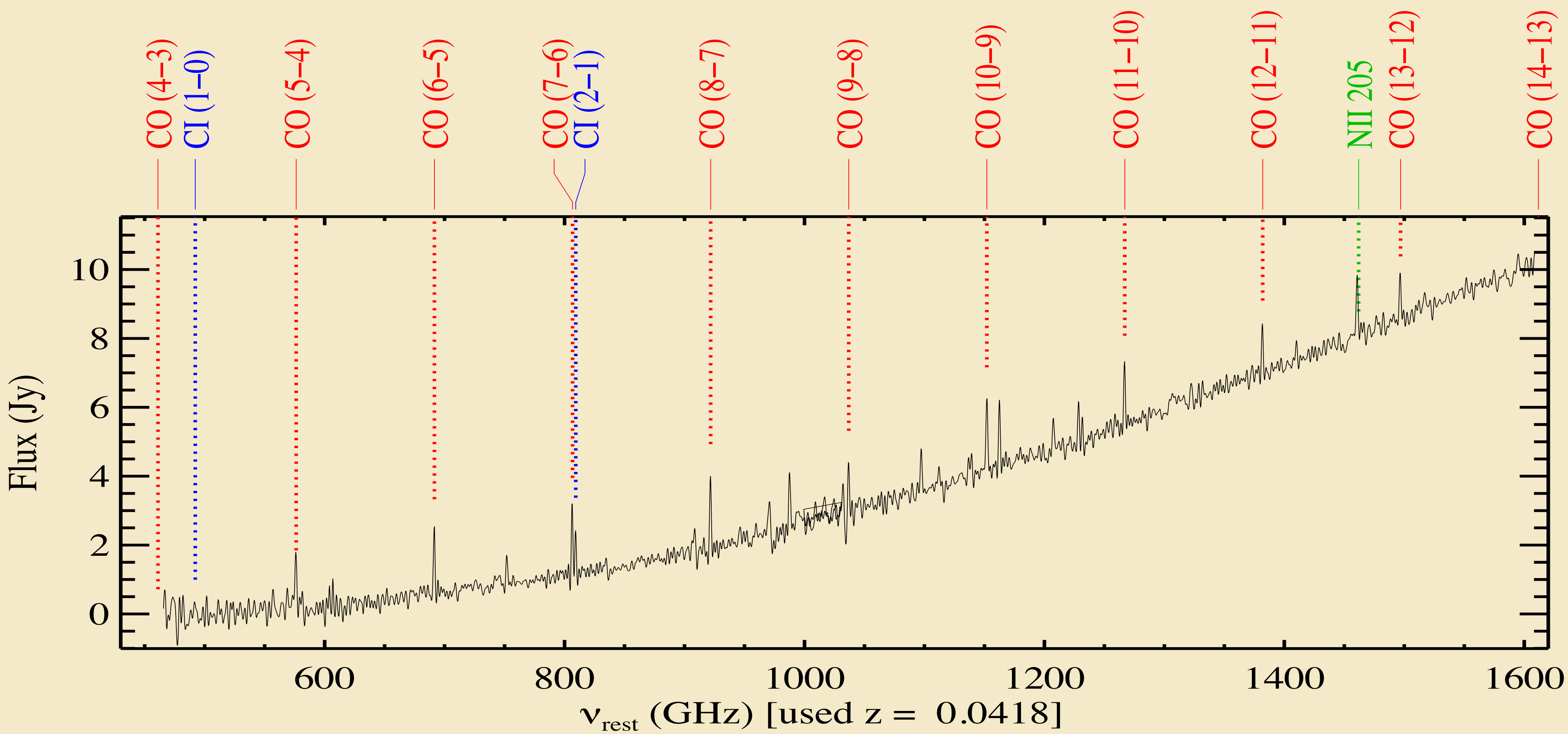

UGC 05101
(LIRG / AGN)

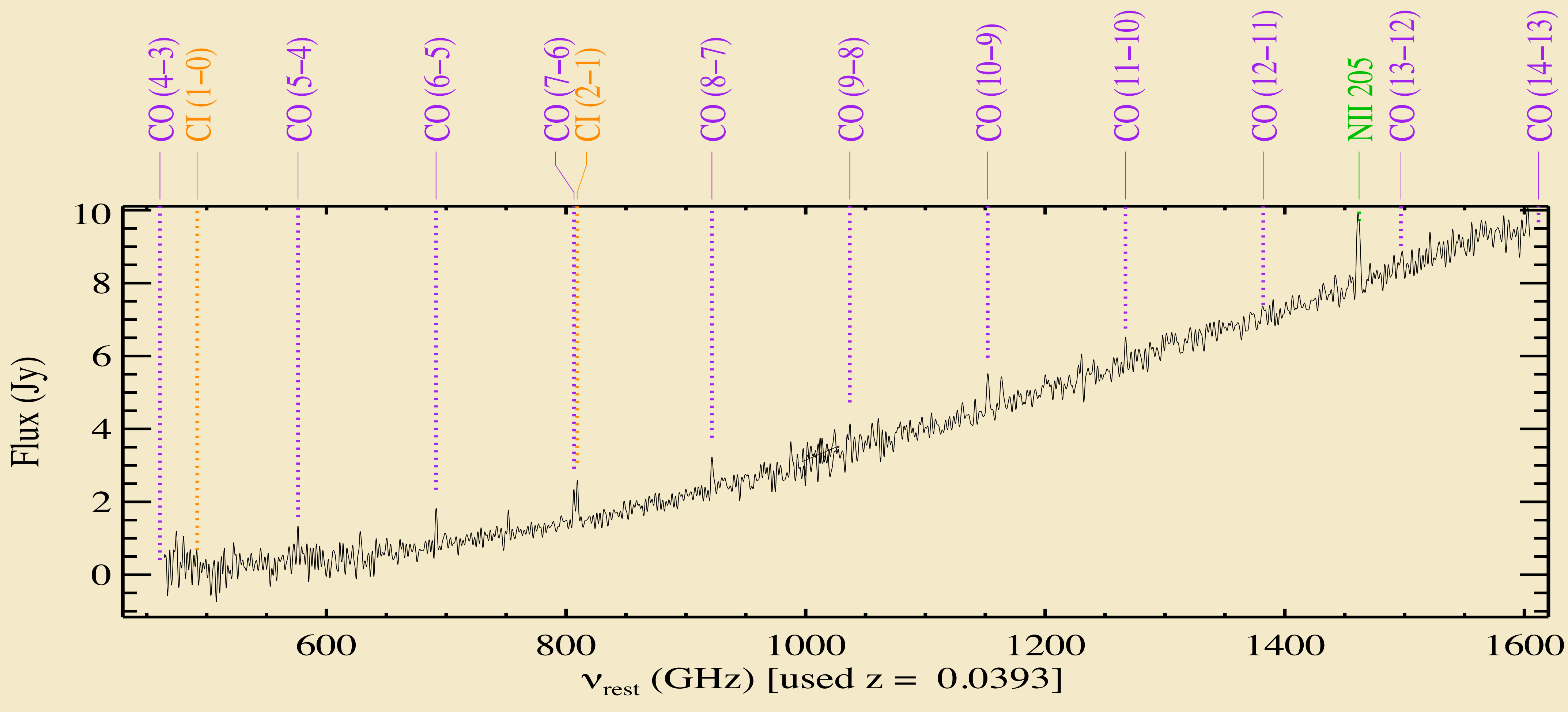

Modeling and Preliminary Results

Non-LTE Radiative Transfer Modeling Arp 220

Rangwala et al. (2011)

— 47 —

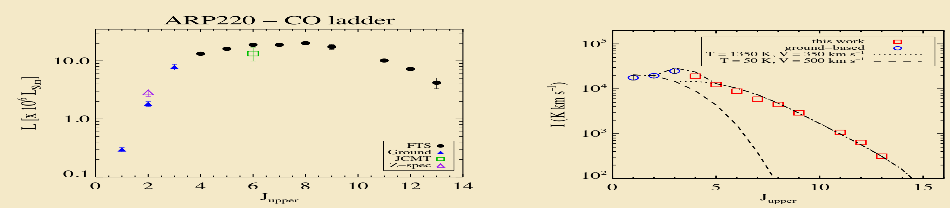

Fig. 5.— Left: Extinction corrected luminosity distribution of the CO ladder from J = 1-0 to J = 13-12 with the exception of J = 10-9 line, which is blended with a water line. The black solid circles are FTS measurements and the blue triangles are average line fluxes from ground-based measurements. Also shown for comparison are new measurements by Z-spec and JCMT. Right: Non-LTE model fit to the observed CO line temperatures. There are two temperature components: a warm component (dotted line) traced by the mid-J to high-J lines and a cold component (dashed line) traced by the low-J lines.

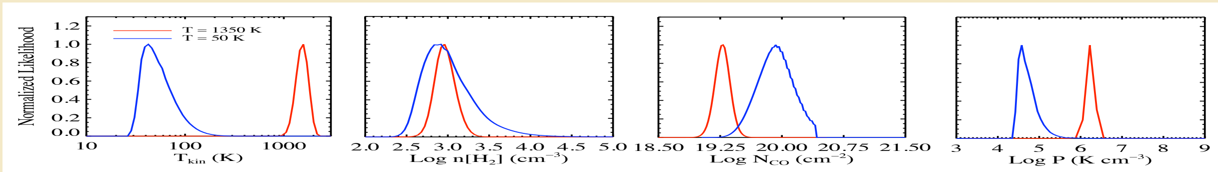

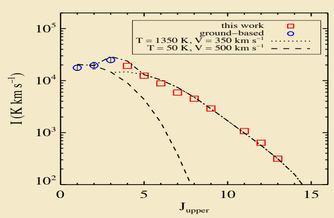

- low-J CO are tracing cold molecular gas
- Mid- to high-J CO are tracing warm gas.
- T_{kin}(warm CO) = T_{kin}(warm H_2)
- M_{gas}(warm) ~ 10% M_{gas}(cold)
- L_{CO}(cold) ~ 8% Total L_{CO}
- cooling rate ~ 22 $L_\odot/M_\odot$

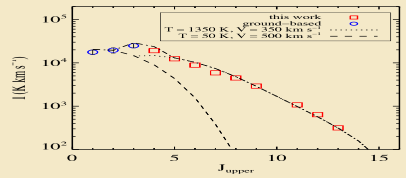

ribution of the CO ladder from J = 1-0
vhich is blended with a water line. The
ue triangles are average line fluxes from
arison are new measurements by Z-spec
ed CO line temperatures. There are two
ted line) traced by the mid-J to high-J
the low-J lines.

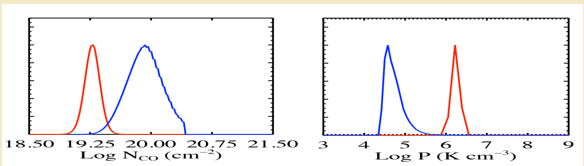

Radiative Transfer code maintained by *Phil Maloney*

Arp 220: Excitation source of warm molecular gas

- Observed ratio: Total $L_{CO}/L_{FIR} \sim 10^{-4}$
- $[T, n(H_2)]_{cold} = [50\ K, 1000\ cm^{-3}]$ and $[T, n(H_2)]_{warm} = [1350\ K, 1000\ cm^{-3}]$
- This ratio along with tight constraints on T_{kin} and $n(H_2)$ rules out PDRs, XDRs and Cosmic ray models
- Require a non-ionizing source of energy: A small fraction of mechanical energy from supernovae and stellar winds can satisfy a cooling rate = 22 $L_\odot/M_\odot$

Similar method has been successfully applied in cases NGC 1068 (*Spinoglio et al. 2012; Hailey-Dunsheath et al. 2012*), M82 (*Kamenetzky et al. 2012*), NGC 4038/39 (*Schirm et al. in prep.*) and Cloverleaf (*Bradford et al. 2009*)

Preliminary

NGC6240: CO Modeling

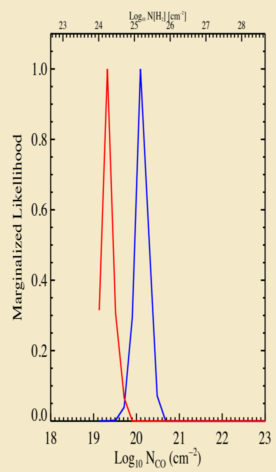

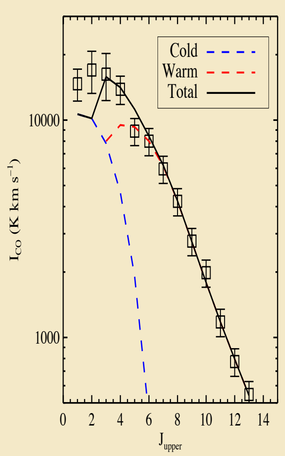

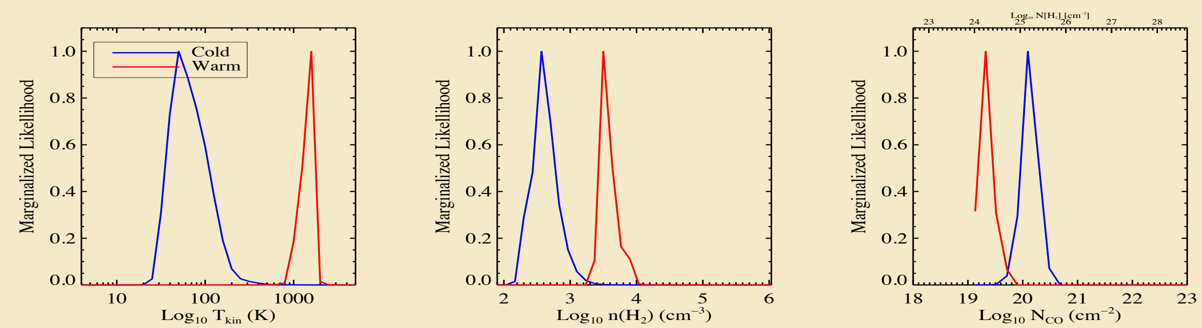

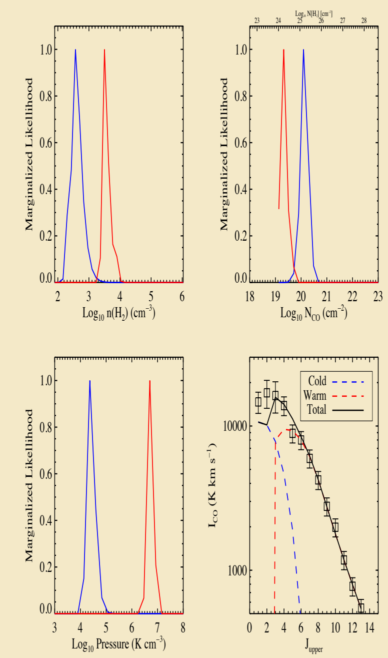

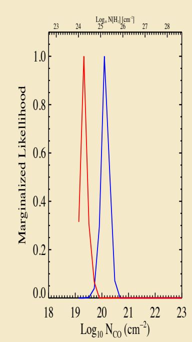

- T_{kin}(warm CO) ~ 1580 K
- T_{kin}(cold CO) ~ 50
- cooling rate ~ 35 $L_{\odot}/M_{\odot}$

Preliminary

M82: CO Modeling Results

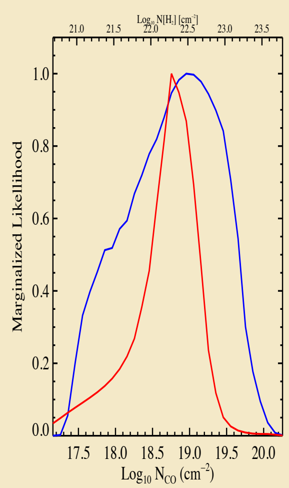

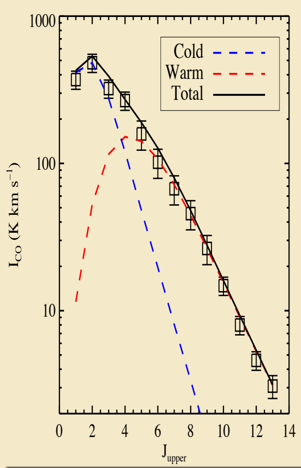

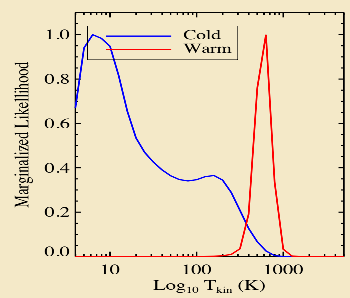

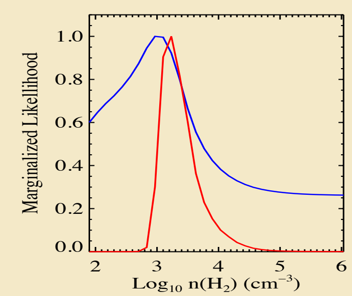

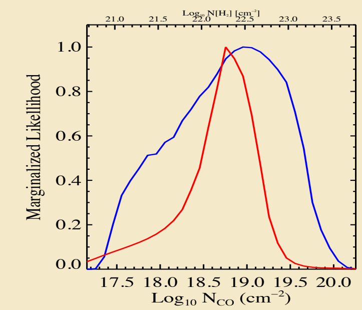

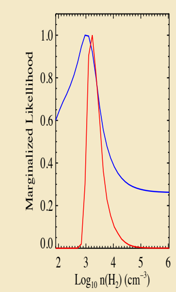

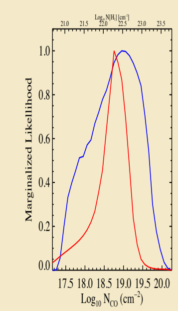

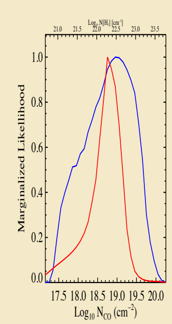

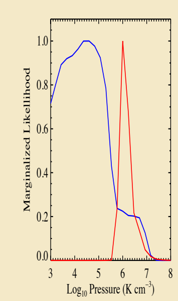

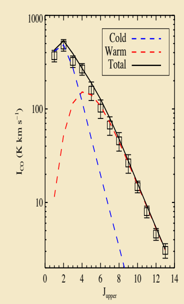

- T_{kin}(warm CO) ~ 500 K = T_{kin}(warm H_2)
- T_{kin}(cold CO) ~ 35 K
- cooling rate ~ 1.4 $L_{\odot}/M_{\odot}$

CO SLEDs

Frequency (GHz)

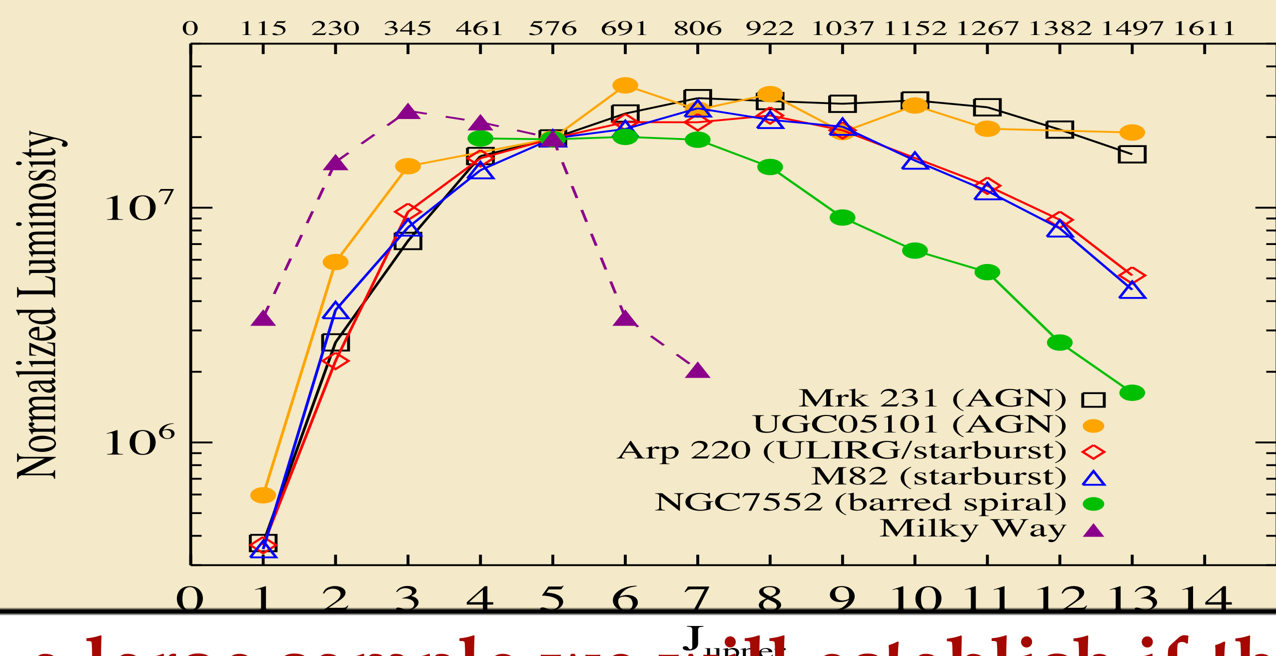

Using a large sample we will establish if the shape and brightness of the CO SLED in galaxies can be used as a diagnostic between dominant sources of energy affecting their molecular ISM and star formation.

Dust Modeling

$$S(\lambda) = \frac{N_{\rm bb}(1 - e^{-\frac{\lambda_0}{\lambda}\beta})(c/\lambda)^3}{e^{\frac{hc}{kT}} - 1} + N_{\rm pl}\lambda^{\alpha}e^{-(\lambda/\lambda_c)^2}$$

Arp220

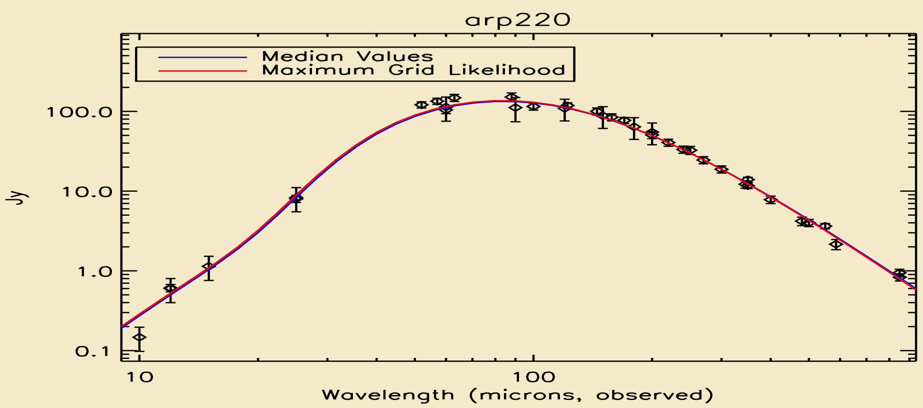

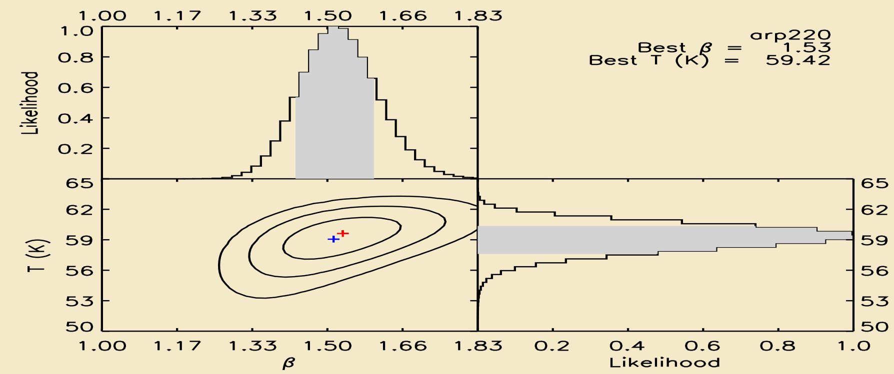

NGC 6240

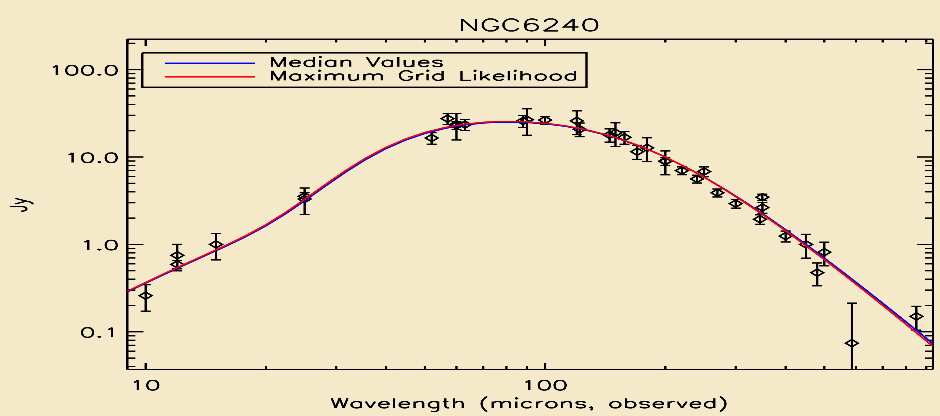

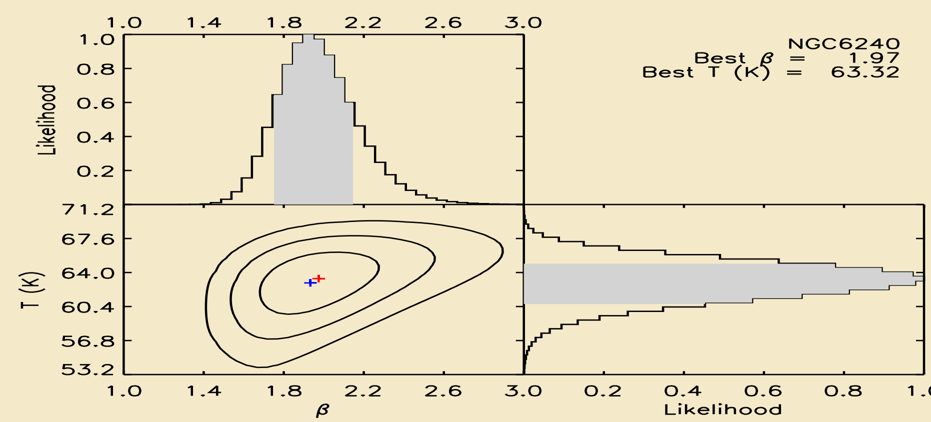

Conclusions

- Molecular gas and dust survey of nearby galaxies using Herschel-SPIRE.

- Systematic re-processing and modeling; Pipeline is almost complete.

- Previous studies have shown that the high-J CO lines are tracing the warm molecular ISM and dominate the CO luminosity and hence the cooling.

- Observed L_{CO}/L_{FIR} combined with physical properties of the molecular gas will enable us to constrain the dominant power source (AGN or SF (PDR, XDR, shocks etc.)) in these galaxies.

- Investigate global properties of the molecular gas and dust as function of L_{FIR} and galaxy types.

Extra Slides

Arp 220: Excitation source of warm molecular gas

- Observed ratio: Total $L_{CO}/L_{FIR} \sim 10^{-4}$
- This ratio along with tight constraints on T_{kin} and $n(H_2)$ rules out PDRs, XDRs and Cosmic rays
- Require a non-ionizing source of energy: Mechanical energy from supernovae and stellar winds to satisfy a cooling rate = 20 $L_{\odot}/M_{\odot}$

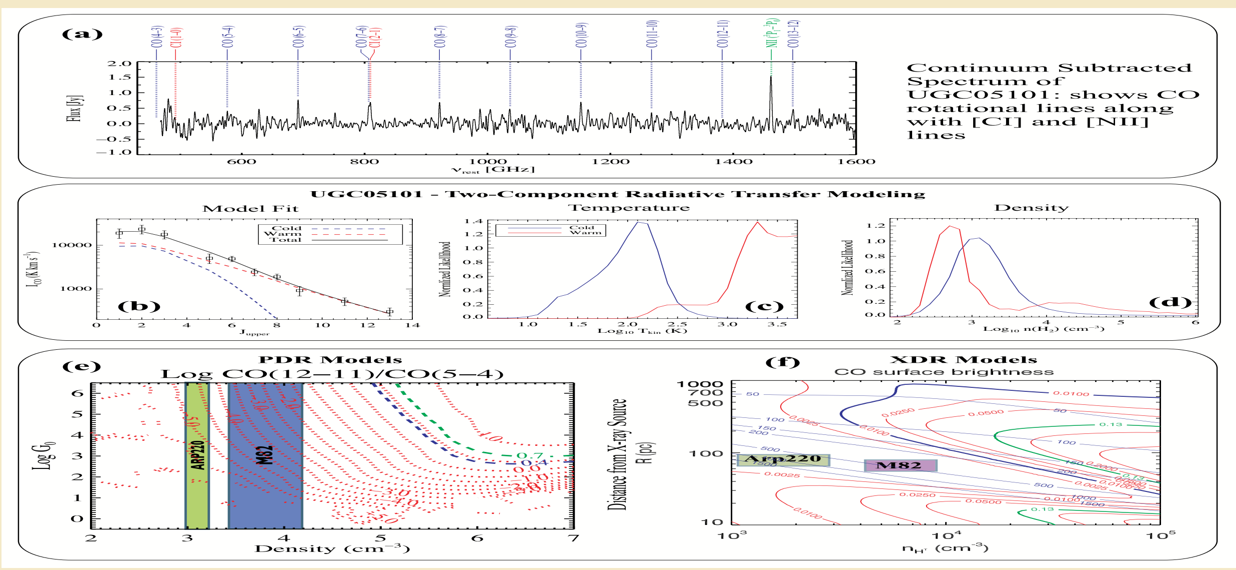

UGC 05101
(LIRG / AGN)

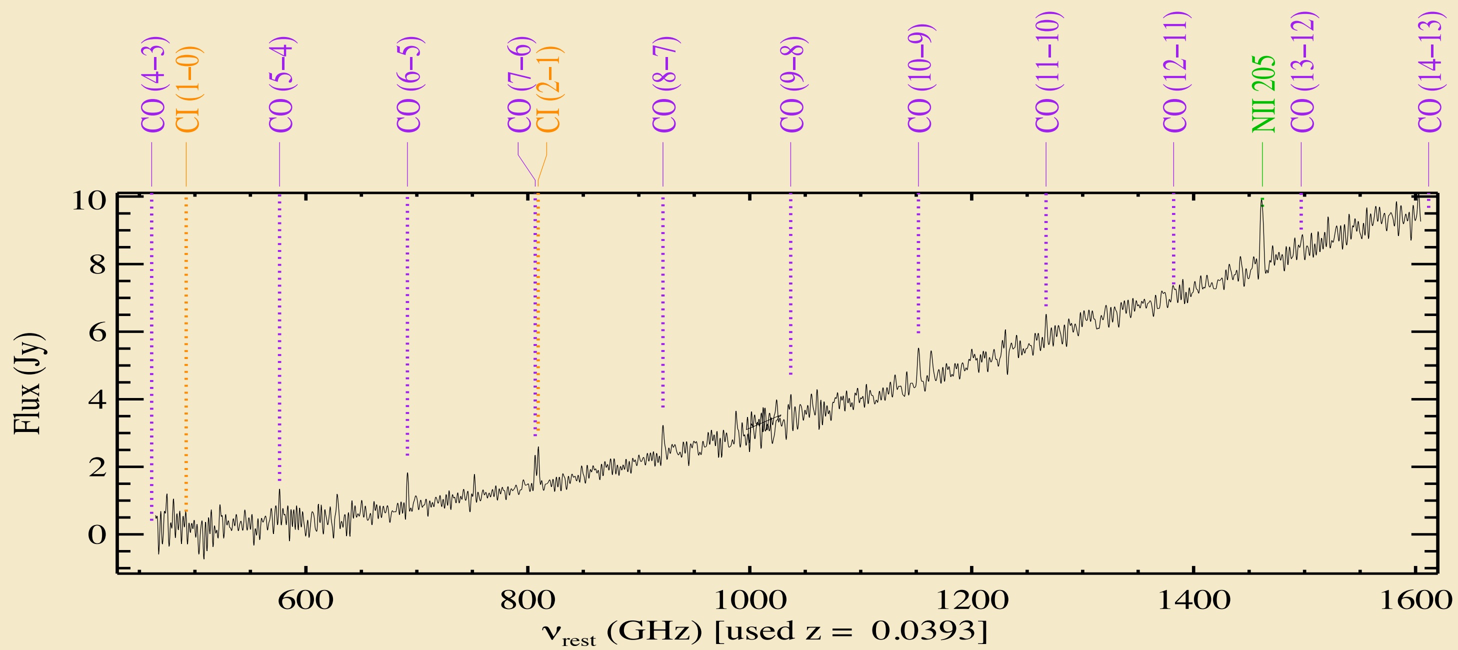

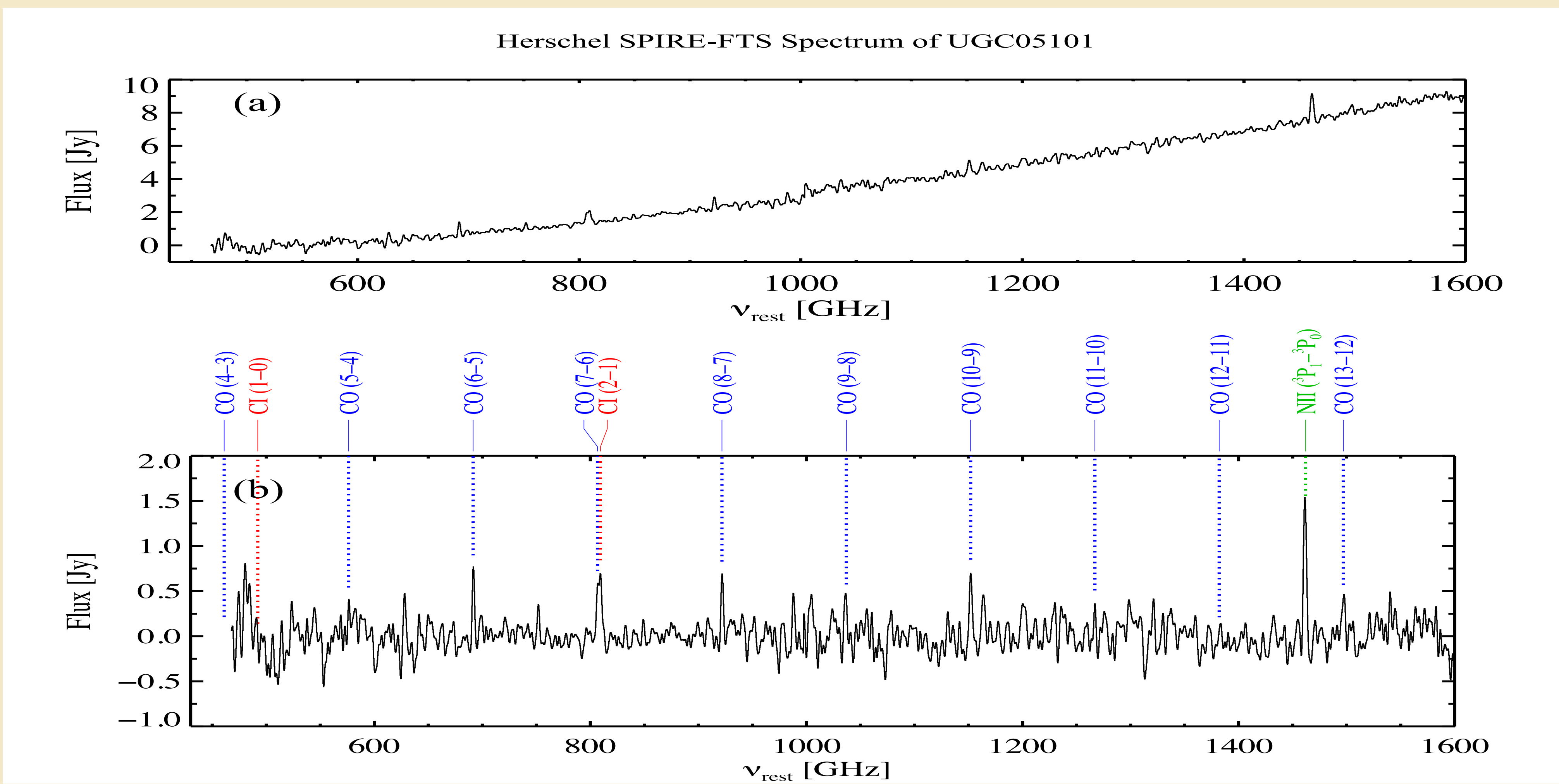

CO SLED: diagnostic for Star Formation Vs AGN?

- Models have suggested that the shape of the CO SLEDs can be used to discriminate between SF and AGN *[e.g. Spaans & Meijerink (2008); Lagos et al. (2012)]*.

- Observations:

  Starburst - CO SLEDs turn over after J = 6-5 e.g. Arp220 [*Rangwala et al. (2011)*] and M82 [*Panuzzo, **Rangwala** et al. (2010); Kamenetzky et al. 2012 (incl. N. Rangwala)*]. Similar turn over observed in high-z submm galaxies *[Bothwell et al. (2013)]*.

- AGN: CO SLED remains flat after J = 6-5 *[e.g.,Van der werf et al. (2010)]*

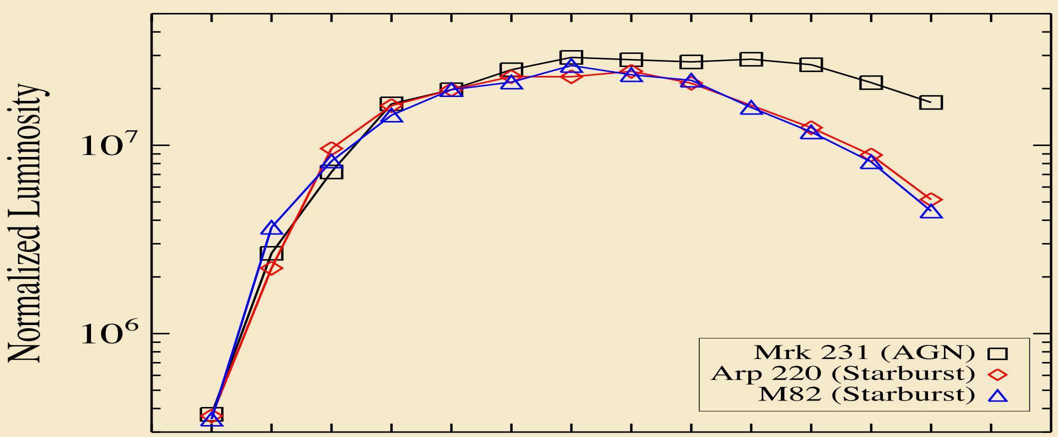

Using a large sample we will establish if the shape and brightness of the CO SLED in galaxies can be used as a diagnostic between dominant sources of energy affecting their molecular ISM and star formation.

LCO - LFIR relation

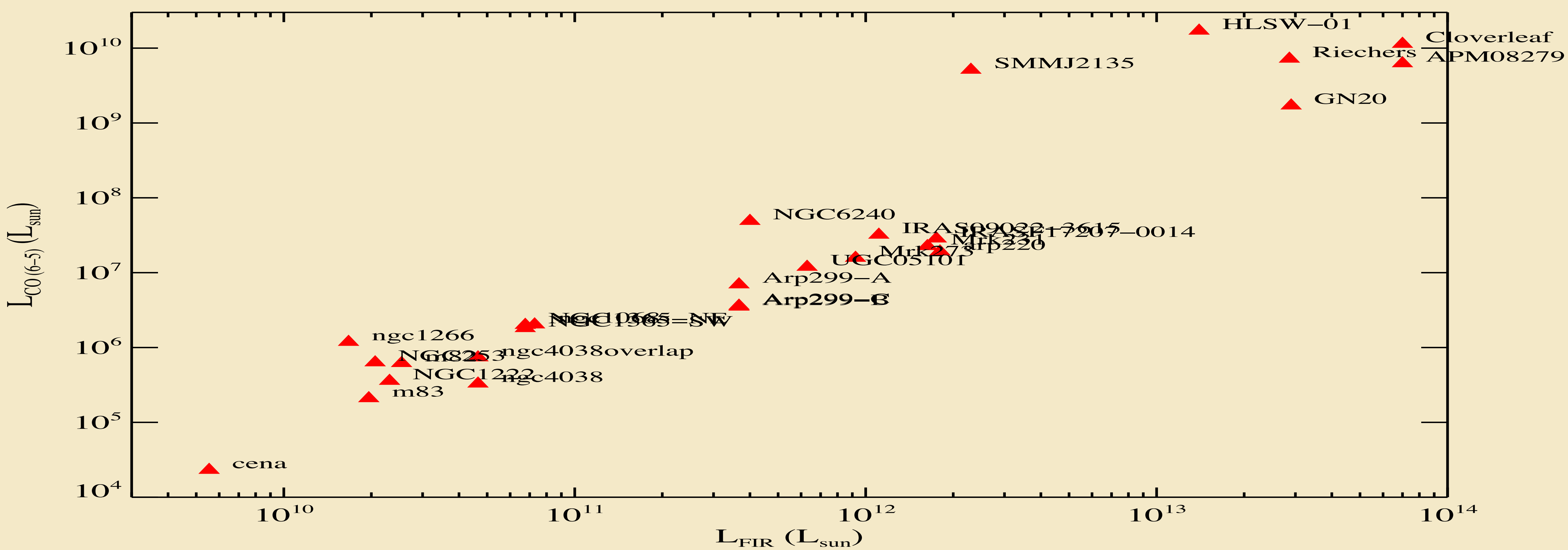

L_{CO} - L_{FIR} relation

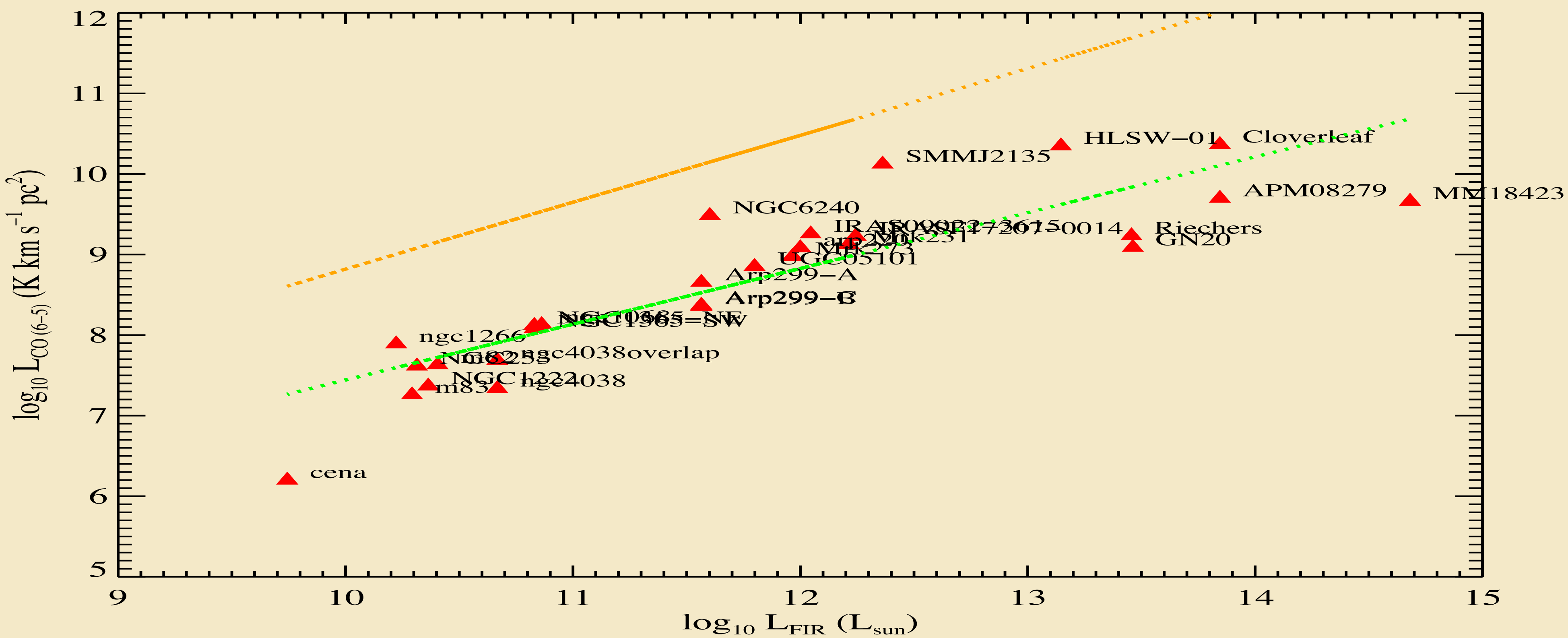

L_{CO} - L_{FIR} relation

4.3 The L'_{CO}–L_{FIR} correlation

A useful quantity to measure for our sample of SMGs is the efficiency with which their molecular gas is being converted into stars. The SFE is sometimes defined as SFR/M(H_2) – the inverse of the gas depletion time – but here we take the approach of parameterizing this as a ratio of observable quantities: L_{FIR} and $L'_{CO(1-0)}$.

There has been debate, in recent years, as to the value of the slope of the $L'_{CO(1-0)} - L_{FIR}$ relation. Whereas, earlier we discussed the difference in slopes between the various transitions observed (in order to derive the median SLED), here we present the relation between the derived ^{12}CO $J = 1$–0 luminosity and L_{FIR} – a relation which describes, in observable terms, the relationship between the luminosity due to star formation and the *total* gas content. (Section 2.1.1 contains a discussion of the uncertainties inherent to deriving IR luminosities for sources such as ours.)

In their study of 12 SMGs, Greve et al. (2005) found a slope of the relation between L_{FIR} and $L'_{CO(1-0)}$ of 0.62 ± 0.08 fit a combined sample of lower redshift LIRGs, ULIRGs and SMGs – identical to the slope derived for the local LIRGs/ULIRGs alone. The small number of galaxies in Greve et al. (2005), however, prevented a full investigation of the SFE slopes within the SMG population itself. Some recent authors, however, have found the slope to be closer to linear – Genzel et al. (2010) found that a slope of 0.87 ± 0.09 fits a combined sample of SMGs across a wide range of redshifts.

Fig. 6 shows the $L'_{CO} - L_{FIR}$ relation for our sample of SMGs. Included in the plot are data points for local (U)LIRGs, as measured by Sanders, Scoville & Soifer (1991) and Solomon et al. (1997). We also show three power-law fits to the local (U)LIRGs alone, the SMGs alone and the combined sample. We find the SMGs to lie slightly above the best-fitting (sub-linear) line for local (U)LIRGs, necessitating a steeper slope. The power-law fit to the local (U)LIRGs alone has a slope of 0.79 ± 0.08, while the fit to the combined sample of SMGs and (U)LIRGs has a slope of 0.83 ± 0.09. It can also be seen that a fit to the SMG sample alone has an even steeper slope of 0.93 ± 0.14 – very close to linear – although, within the uncertainty, this is consistent with the slope for the combined samples. These results are in good agreement with most previous findings; the near-linear slopes (which agree well with those found by Genzel et al. 2010) would imply a roughly constant gas depletion time-scale across the entire range of far-IR luminosities shown here.

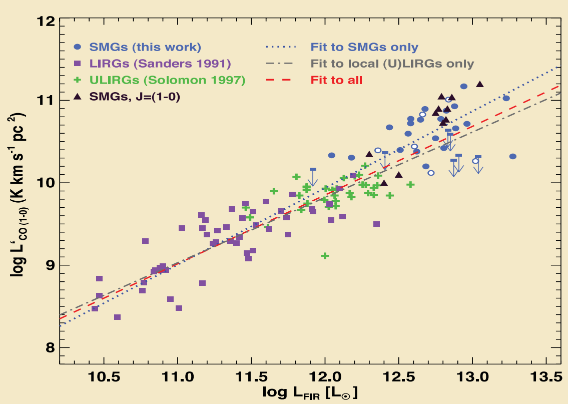

Figure 6. The SFE, L'_{CO} versus L_{FIR}. Included in the plot are two samples of local ULIRGs, and the $J = (1$–0) SMG observations of Ivison et al. (2011). Best-fitting slopes to the SMGs alone, the local ULIRGs alone and all three combined samples are overplotted. They have slopes of 0.93 ± 0.14, 0.79 ± 0.08 and 0.83 ± 0.09, respectively.

However, we caution that our analysis requires extrapolating from high-J_{up} ^{12}CO transitions to ^{12}CO (1–0). Ivison et al. (2010) have undertaken a similar analysis based solely on directly observed ^{12}CO (1–0) observations and homogeneously derived far-IR luminosities and conclude that the $L'_{CO(1-0)} - L_{FIR}$ relation has a slope substantially below unity. We therefore suggest that it is difficult to draw any strong conclusions from high-J_{up} observations about the gas depletion time-scales of the different populations or the form of the Kennicutt–Schmidt relation in these galaxies, as these are too uncertain without brightness temperature ratio measurements for individual sources.

4.4 Molecular gas masses

Part of the power of observations of ^{12}CO emission from high-redshift galaxies is that they provide a tool to derive the mass of the reservoir of molecular gas in these systems. This is of critical importance because this reservoir is the raw material from which the future stellar mass in these systems is formed. Along with the existing stellar population, it therefore gives some indication of the potential stellar mass of the resulting galaxy at the end of the starburst phase (subject, of course, to the unknown contribution from in-falling and out-flowing material).

Estimating the mass of H_2 from the measured L'_{CO} requires two steps. First, luminosities originating from higher transitions ($J_{up} \geq 2$) must be transformed to an equivalent ^{12}CO $J = 1$–0 luminosity, using a brightness ratio. We have derived the necessary brightness ratios using our composite SLED as discussed in Section 3 above. Once an $L'_{CO(1-0)}$ has been determined, it must be converted into an H_2 mass by adopting a conversion factor α: $M(H_2) = \alpha L'_{CO}$, where α is in units of $M_\odot$ (K km s^{-1} pc^2)$^{-1}$ (when discussing α hereafter, we omit these units for the sake of brevity). This can then be converted to a total gas mass, including He, $M_{gas} = 1.36\, M(H_2)$.

There is a large body of work, both observational and theoretical, dedicated to determining the value – and ascertaining the metallicity or environmental dependence – of α (e.g. Young & Scoville 1991; Solomon & Vanden Bout 2005; Liszt, Pety & Lucas 2010; Bolatto et al. 2011; Genzel et al. 2012; Narayanan et al. 2011; Papadopoulos et al. 2012). While secular discs such as the Milky Way have a relatively 'high' value of $\alpha \sim 3$–5, using this value for the gas in nuclear discs/rings within merging systems and starbursts at $z \sim 0$ leads to the molecular gas mass sometimes exceeding their dynamical masses. As such, a lower value – motivated by a radiative transfer model of the ^{12}CO kinematics – is typically used for the intense nuclear starbursts in the most IR-luminous local systems: $\alpha \sim 0.8$, with a range of 0.3–1.3 (Downes & Solomon 1998). However, some recent results have suggested that this value might, in fact, *underestimate* the true value in high-redshift SMGs. Bothwell et al. (2010) found that applying the canonical ULIRG value to two $z \sim 2$ SMGs resulted in gas fractions of <10 per cent, which appears incongruous given their extreme SFRs. Similarly, a dynamical analysis has been undertaken on the high-redshift SMG, SMM J2135−0102, by Swinbank et al. (2011) yielding a higher value, $\alpha \sim 2$ [supported by Large Velocity Gradient (LVG) modelling; Danielson et al. 2011].

Here we adopt a value of $\alpha = 1.0$, and caution that all gas masses derived are dependent on this uncertain parameter. Using this value, the resulting mean H_2 mass of our sample SMGs (including limits

Bothwell et al. (2013)

SPIRE-FTS spectrum of Arp 220

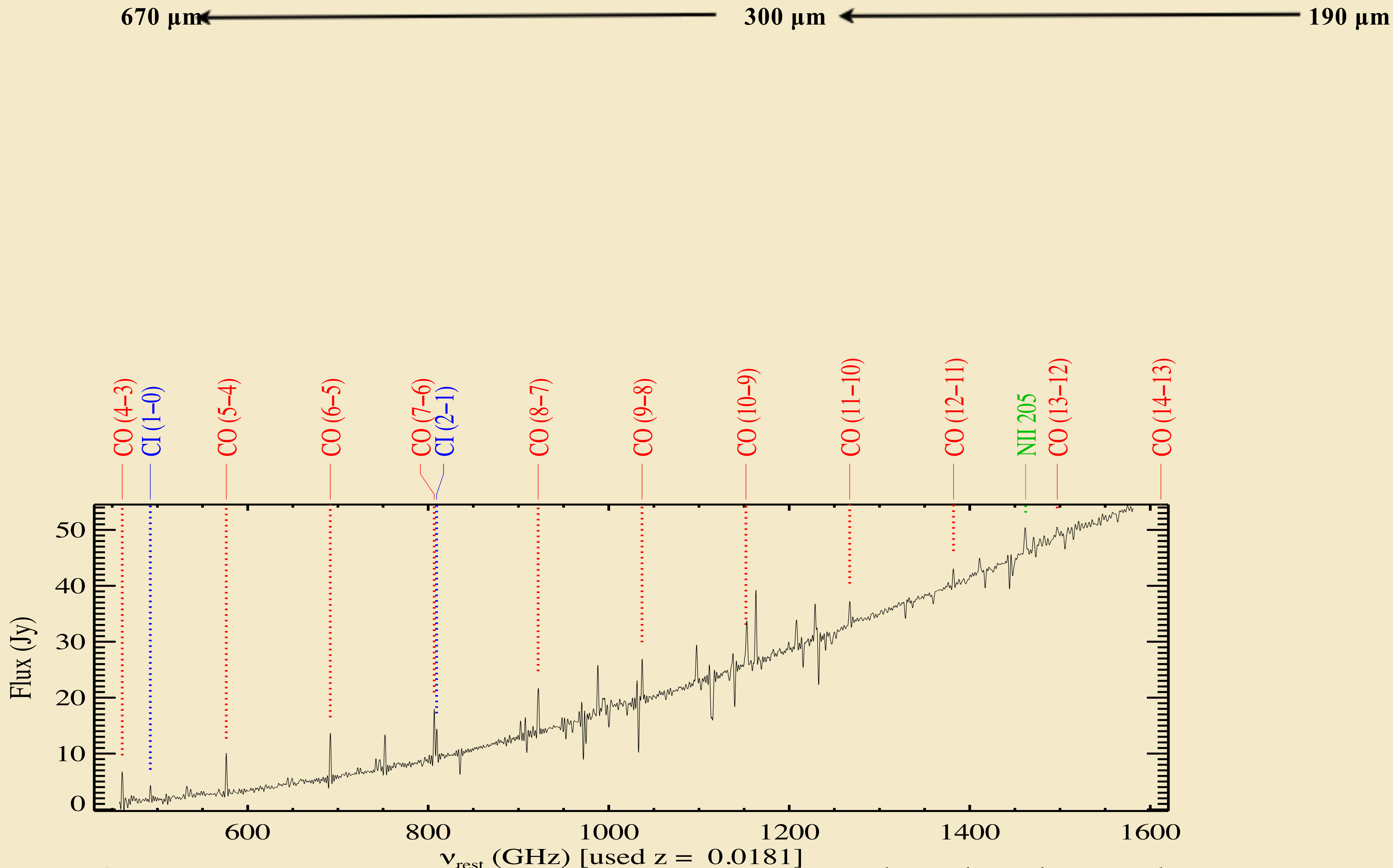

- Continuous spectral coverage
- spectral resolution = 1.44 GHz
- several molecular and atomic species
- CO rotational transitions from J = 4-3 to 13-12